Grain-size-sensitive deformation of upper greenschist- to lower amphibolite-facies metacherts from a low-*P*/high-*T* metamorphic belt

Takamoto Okudaira[a], Daisuke Ogawa[a], Katsuyoshi Michibayashi[b]

[a]*Department of Geosciences, Osaka City University, Osaka 558-8585, Japan*

[b]*Geological Institute, Shizuoka University, Shizuoka 422-8529, Japan*

Corresponding author. Fax: +81 6 6605 2522. *E-mail address:* oku@sci.osaka-cu.ac.jp (T. Okudaira)

Keywords: Diffusion creep, Grain-size-sensitive flow, Metachert, Ryoke metamorphic belt, Lattice-preferred orientation

ABSTRACT

To identify the dominant deformation mechanism in continental middle crust at an arc–trench system, we used an SEM-EBSD system to measure the lattice-preferred orientations of quartz grains in fine-grained metachert from the low-grade (chlorite and chlorite–biotite zones) part of the low-*P*/high-*T* Ryoke metamorphic belt, SW Japan. Quartz *c*-axis fabrics show no distinct patterns related to dislocation creep, although the strain magnitudes estimated based on deformed radiolarian fossils are high enough that a distinct fabric might be expected to have formed during deformation. Fabric intensities are very low, indicating a random distribution of quartz *c*-axes. Quartz grains are equant in shape and polygonal, and free of intracrystalline plasticity. These observations suggest that the dominant deformation mechanism in the metacherts was grain-size-sensitive flow (diffusion creep accompanied by grain-boundary sliding) rather than dislocation creep, possibly reflecting the relatively low strain rate or low flow stress compared with that in high-strain zones. The development of grain-size-sensitive flow in metamorphic tectonites at mid-crustal conditions would result in a significant decrease of the rocks strength of the continental middle crust.

1. Introduction

The dominant deformation mechanism within metamorphic tectonites is the most important factor in understanding the rheological behavior of the crust and mantle, as the effective viscosity is markedly different for rocks deformed by dislocation creep or grain-size-sensitive flow (diffusion creep accompanied by grain-boundary sliding or

diffusion accommodated grain-boundary sliding). In dislocation creep, the strain rate is independent of grain size but has a strong non-linear dependence on flow stress. In grain-size-sensitive creep, in contrast, strain rate has a linear dependence on stress but a non-linear dependence on grain size. Grain size appears to be the main parameter in determining whether an aggregate deforms by dislocation creep or by grain-size-sensitive creep associated with diffusive mass transfer within crystals or along grain boundaries (e.g. Schmid et al., 1977; Etheridge and Wilkie, 1979; Behrmann, 1983). Small grain size favors grain-size-sensitive creep, as diffusion paths are relatively short. The presence of a second mineral phase can enhance this process because it inhibits syn-deformation grain growth keeping the grains small enough so that grain-size-sensitive creep can be active (e.g. Herwegh and Jenni, 2001; Krabbendam et al., 2003; Herwegh and Berger, 2004; Song and Ree, 2007).

The flow laws for grain-boundary diffusion creep (Coble creep) and diffusion accommodated grain-boundary sliding have a similar dependence on flow stress (stress exponent ~1) and grain size (grain-size exponent ~3) so the mechanisms cannot be distinguished from these exponents alone. In this study, Coble creep will be used to describe grain-size-sensitive creep. According to Passchier and Trouw (2005; p. 65), for a quartz aggregate, the flow law for bulk diffusion-controlled dislocation creep can be expressed by

$$\dot{\varepsilon} = \frac{\mu b D_L}{\mathrm{k}T} \cdot (\sigma/\mu)^3 \cdot e^{(-H_L/\mathrm{R}T)}, \qquad (1)$$

and the flow law for Coble creep is

$$\dot{\varepsilon} = \frac{A_C \mu V D_G W}{\mathrm{R}Td^3} \cdot (\sigma/\mu) \cdot e^{(-H_G/\mathrm{R}T)}, \quad (2)$$

where $\dot{\varepsilon}$ is strain rate [s^{-1}]; σ is flow stress [Pa]; T is temperature [K]; b is the Burgers vector [m]; A_C is a numerical factor for Coble creep, which depends on grain shape and boundary conditions (141); H_L and D_L are molar activation enthalpy (243 kJ/mol) and pre-exponential factor (2.9 x 10^{-5} m^2/s) for oxygen self-diffusion used in the flow law for dislocation creep (Farver and Yund, 1991); H_G and D_G are molar activation enthalpy (137 kJ/mol) and pre-exponential factor (3.7 x 10^{-10} m^2/s) for silicon bulk diffusion in the presence of water for diffusion creep (Farver and Yund, 2000); W is grain-boundary thickness (10^{-7} m); V is the molar volume of quartz (2.6 x 10^{-5} m^3/mol); μ is the shear modulus of quartz (42 x 10^9 Pa); d is grain size [m]; R is a gas constant (8.3143 J/mol/K); and k is the Boltzmann constant (1.38062 x 10^{-23} J/mol/K). The effective viscosity η, that is calculated using Eqs. (1) and (2), the relationship $\eta = \sigma/\dot{\varepsilon}$ and assuming $\dot{\varepsilon}$ = 10^{-14} s^{-1}, of a quartz aggregate deforming by dislocation creep at 500 °C is approximately three orders of magnitude higher than that of an aggregate (grain size, 10 μm) deforming by diffusion creep (Fig. 1).

Previous studies have reported the deformation of various rock types (e.g. marbles, peridotites and granitic mylonites) by grain-size-sensitive flow (e.g. Schmid et al., 1977; Lisle, 1985a; Behrmann and Mainprice, 1987; Stünitz and Fitz Gerald, 1993; Rutter et

al., 1994; Fliervoet et al., 1997; Kruse and Stünitz, 1999; Jiang et al., 2000; Bestmann and Prior, 2003; Herwegh and Berger, 2004; Storey and Prior, 2005; Warren and Hirth, 2006). In contrast, although a few papers reported grain-size-sensitive flow in quartz aggregates (e.g., Krabbendam et al., 2003; Wightman et al., 2006; Song and Ree, 2007), almost all quartzose rocks (e.g. quartzites and quartz mylonites) are considered to deform by dislocation creep, even in ultrafine-grained rocks (Fliervoet and White, 1995; Rutter and Brodie, 2004; Fitz Gerald et al., 2006; Ishii et al., 2007).

The low-*P*/high-*T* metamorphic rocks of the Cretaceous Ryoke metamorphic belt, SW Japan, are considered to be derived from the Jurassic Mino–Tamba accretionary complex (e.g. Okudaira et al., 2009). Because accretionary complexes form at a subduction zone and low-*P*/high-*T* metamorphic belts form near a volcanic arc, the deformation history of metamorphosed accretionary complexes (e.g. the Ryoke metamorphic belt) represents a key to understanding the nature of geodynamic processes in continental middle crust.

In studies of low-grade (chlorite–biotite and biotite zones) metacherts of the Ryoke metamorphic belt, Toriumi et al. (1986) and Toriumi (1989) reported microstructures that could not have originated by dislocation glide. Although their microstructural and textural analyses were not sufficient, they suggested that the rocks deformed by diffusive mass transfer, including pressure solution, under low flow stress or a low strain rate. On the other hand, it has been suggested that in high-grade (cordierite, sillimanite and garnet–cordierite zones) metacherts dislocation creep is the dominant deformation mechanism (Hara, 1962; Okudaira et al., 1995).

In the present study, we used a scanning electron microscope (SEM) equipped with electron backscatter diffraction (EBSD) to analyze the lattice-preferred orientations (LPOs) of quartz grains in very-fine-grained metacherts from the Ryoke metamorphic belt, with the aim of clarifying the effects of physical parameters on the development of grain-size-sensitive creep within fine-grained metamorphic tectonites.

2. Methods and results

2.1. Samples

In the Wazuka-Kasagi district, SW Japan, non-metamorphosed sedimentary rocks of the Mino–Tamba accretionary complex show a gradual transition to Ryoke metamorphic rocks (Fig. 2). The metamorphic rocks are divided into the following four mineral zones (in order of increasing metamorphic grade): chlorite zone, chlorite–biotite zone, biotite zone, and sillimanite zone (Ozaki et al., 2000). The chlorite and chlorite-biotite zones are of upper greenschist to lower amphibolite facies; the metamorphic temperature of the chlorite–biotite zone in this area has been estimated to be ≤490 °C, based on the occurrence of fully ordered graphite in the highest-grade rocks of this zone (Nakamura, 1995). The samples of metachert analyzed in the present study were collected from the chlorite zone (sample 080429-04) and chlorite-biotite zone (sample 070523-12). The samples exhibit banding structures defined by alternating thick (several centimeters) chert layers and thin (several millimeters) pelitic layers oriented parallel/subparallel to lithologic boundaries. Numerous deformed radiolarian fossils (average diameter ~200 μm) are observed; the fossils can be recognized based on

their ellipsoidal and rounded shapes. The long axes of the fossils are aligned to define a weak tectonic foliation (Fig. 3a). The fossils are filled with quartz grains larger than the matrix ones. Quartz grains within the fossils are polygonal, with no shape-preferred orientation. A schistosity develops within thin pelitic layers that also include deformed radiolarian fossils. A weak stretching lineation is observed upon the schistosity. The metacherts are not folded mesoscopically. For strain and fabric analyses, thin sections were prepared normal to the schistosity and parallel to the stretching lineation (*XZ*-sections), normal to both the schistosity and the lineation (*YZ*-sections), and parallel to the schistosity (*XY*-sections).

2.2. Microstructures

The chlorite zone sample consists mainly of quartz, with minor muscovite, chlorite, graphite, pyrrhotite and ilmenite. The chlorite–biotite zone sample consists of quartz, with minor muscovite, chlorite, biotite, graphite, pyrrhotite and ilmenite. Quartz grains in the matrix are largely equigranular in both samples and exhibit foam-like microstructure (Fig. 3b, c), although some are elongated subparallel to the lineation, defining a weak tectonic foliation. There are no microstructures indicative of dynamic recrystallization (e.g. undulose extinction or grain-boundary bulging). The minor sheet silicates are not clustered, and they commonly occur along quartz grain boundaries, having a strong preferred orientation with the basal planes parallel to the tectonic foliation. They exhibit no chemical heterogeneity within each crystal.

The grain sizes and modal percentages of quartz grains were estimated by image

analysis using the software NIH image. Grain sizes were calculated as the equivalent diameter of a spherical grain. Table 1 lists the average grain sizes and modal percentages of quartz grains for that part of sample 080429-04 from which LPO data were measured, and for four domains exhibiting different grain size of quartz within sample 070523-12. Average quartz grain sizes of the chlorite zone metachert (080429-04) and domains of smaller grain size in the chlorite-biotite zone sample (070523-12) are ~10 μm, whereas those of domains of larger grain size in the chlorite-biotite zone sample are ~20 μm. The modal abundance of quartz in the chlorite-biotite zone metachert varies slightly depending on different domains: it is lower in the domains of smaller quartz grain size (Table 1).

2.3. Strain magnitude

Deformed radiolarian fossils serve as good strain makers in studies of deformation within low- to medium-grade metacherts because strains in pure metacherts are reasonably homogeneous; i.e., the radiolarian fossils and matrix record the same strain (e.g., Toriumi et al., 1988). It has been considered that the radiolarian fossils and surrounding matrix were deformed mainly during the low-*P*/high-*T* Ryoke metamorphism, because radiolarian fossils in the Mino–Tamba accretionary complex are sufficiently well preserved that they are easily identified to the species level (Toriumi et al., 1986, 1988; Toriumi, 1989; Fukui and Kano, 2007; Okudaira et al., 2009). To analyze the strain recorded by metacherts, we applied the R_f–ϕ method (Dunnet, 1969; Dunnet and Siddans, 1971; Ramsay and Huber, 1983) to the deformed

radiolarian fossils. In this analysis, we assume that when the rocks deform, elliptical passive markers are transformed to new elliptical markers with an ellipticity (i.e., aspect ratio, R_f) and long-axis orientation ϕ that depend on the original shape (R_i) and orientation (θ) of the marker ellipses in addition to the shape (R_s) and orientation of the strain ellipse. We evaluated the shape of the strain ellipses R_{XY}, R_{XZ}, and R_{YZ} on each of the *XY*-, *XZ*-, and *YZ*-planes using the R_f–ϕ method, respectively (Fig. 4).

In the case of constant-volume deformation, the magnitude of strain ($\bar{\varepsilon}_s$) can be calculated as the quadratic mean of the principal natural strains using the following equation (Nadai, 1963; Ramsay and Huber, 1983):

$$\bar{\varepsilon}_s = \frac{1}{\sqrt{3}}\left\{\left(\ln R_{XY}\right)^2 + \left(\ln R_{XZ}\right)^2 + \left(\ln R_{YZ}\right)^2\right\}^{1/2} \quad (3).$$

We obtained the natural strain magnitudes of 0.69 and 0.60 for sample 080429-04 and sample 070523-12, respectively, with these strain magnitudes being comparable with values obtained for other metacherts in the district (~0.6–0.7; Okudaira et al., 2009).

2.4. Lattice-preferred orientation

We used electron backscatter diffraction (EBSD: e.g., Prior et al., 1999) to measure the lattice orientations of quartz crystals in *XZ*-sections. Data were collected using an EBSD system attached to an SEM (JEOL JSM-6300) housed at the Centre for Instrumental Analysis, Shizuoka University, Japan. Operating conditions were as follows: accelerating voltage of 20 kV, probe current of 10 nA, working distance of 24 mm, and

specimens tilted at 70°. We measured the crystal orientations of 200–300 quartz grains per small domain(s) in sample, visually checking the computerized indexation of each diffraction pattern that was manually picked up by moving the beam from grain to grain. All index data represent points with a mean angular deviation (MAD) of <1°.

Figure 5 shows pole figures of the measured quartz *c*-axis fabrics. The pole figures show weak fabrics (e.g. small girdle patterns or type I crossed girdles; e.g. Lister and Hobbs, 1980), but no distinct patterns that are predicted theoretically or experimentally. We calculated the fabric strength for each pole figure based on the fabric intensity, as proposed by Lisle (1985b) and Woodcock and Naylor (1983). Related to the fabric intensity, it is possible to calculate significance levels for the uniformity statistic S_u (Lisle, 1985b). Data that yield low S_u values are suspect on the grounds of being too uniform for a random sample. Values of fabric intensity and S_u determined in the present study are listed in Table 1. The S_u values are less than 11.07 (the 95% level of significance; except for domains 3 and 4 in sample 070523-12), indicating uniform distributions.

Figure 6 shows the distributions of uncorrelated misorientation angles for each analysis, as calculated from the complete set of all possible grain pairs, including those not in direct contact (Wheeler et al., 2001). For a strong fabric, many grains have similar orientations; consequently, the distribution of misorientation angles is dominated by small angles. The measured distributions are similar to the theoretical curve for a random fabric, suggesting that the quartz fabrics are very weak. We also calculated the fabric intensity for each quartz fabric based on the M-index (Skemer et al.,

2005), which represents the difference between the measured and theoretical uncorrelated misorientation angles. Individual misorientation angles were calculated from EBSD data. The calculated M-index values are 0.053 for sample 080429-04, and for sample 070523-12, 0.060 (domain 1), 0.067 (domain 2), 0.066 (domain 3) and 0.074 (domain 4) (see also Table 1).

3. Discussion

3.1. Deformation mechanism of metacherts

Our EBSD analyses revealed weak quartz fabrics. Based on a numerical simulation of fabric development in quartzite, a visible fabric pattern develops after a strain of ~0.3 and that the fabric intensity increases with increasing strain (Lister and Hobbs, 1980; Jessell, 1988; Wenk et al., 1989; Takeshita et al., 1999). In the present study, an analysis of deformed radiolarian fossils within the metacherts indicated a natural strain of ~0.7; on this basis, the samples would be expected to show distinct quartz fabric patterns, possibly indicating dislocation creep as the dominant deformation mechanism. However, diffusion creep combined with grain-boundary sliding may prevent the development or cause the destruction of an existing lattice-preferred orientation. If a fine-grained mineral aggregate has undergone high strain but consists of equant grains, lacking a clear lattice-preferred orientation, or has a lattice-preferred orientation that cannot be explained by dislocation creep, it might be inferred that diffusion creep accompanied by grain-boundary sliding was the dominant deformation mechanism (e.g. Rutter and Brodie, 2004).

The equant quartz grains in the analyzed metacherts (Fig. 3) may have formed during deformation. Although the observed foam-like microstructure indicates significant annealing and/or grain growth subsequent to shear deformation, previous studies have proposed that grain growth in itself does not destroy a LPO (Heilbronner and Tullis, 2002; Otani and Wallis, 2006); it may even enhance an LPO fabric because of the selective growth of grains in a preferred orientation (Neumann, 2000). In fact, previous transmission electron microscope (TEM) studies of the low-grade metacherts from the Ryoke metamorphic belt (Toriumi et al., 1986; Toriumi, 1989) have revealed that dislocations are homogeneously distributed within quartz grains at a density up to about 10^8 cm^{-2}, with no dislocation walls or bowed-out dislocations. These observations suggest the foam-like microstructure was not formed by annealing subsequent to dislocation creep deformation, as annealing following dislocation creep would have produced dislocation walls.

Fabric intensities of quartz aggregates with large grain size are on the whole higher than those with small grain size (Fig. 7), suggesting that the importance of dislocation creep, in terms of bulk deformation, increases with increasing quartz grain size. This finding may suggest that deformation of the very-fine-grained metacherts was associated with intracrystalline dislocation activity as an accommodation mechanism. Dislocation-accommodated grain-boundary sliding is a grain-sensitive creep mechanism that possibly occurs in various materials (e.g. silicates, carbonates and ice) deformed at the transition between dislocation creep and diffusion creep (e.g. Rutter et al., 1994; Hirth and Kohlstedt, 1995; Goldsby et al., 2001; Herwegh and Jenni, 2001;

Krabbendam et al., 2003; Herwegh and Berger, 2004; Warren and Hirth, 2006; Barreiro et al., 2007; Song and Ree, 2007; Delle Piane et al., 2009). In this mechanism, strain is accommodated mainly by the relative movement of grains (i.e. grain-boundary sliding) and is limited by either this process or the movement of dislocations upon a readily activated slip system. These two processes act together, as deformation is not independently accommodated by either grain-boundary sliding or easy slip (Etheridge and Wilkie, 1979; De Bresser et al., 2001). Such deformation has been shown to produce weak LPOs.

Quartz grains in metacherts of the chlorite and chlorite-biotite zones are very fine, that can be comparable to those of ultramylonites. The reason why the small grain size of quartz under the condition of upper greenschist- to lower amphibolite-facies may be resulted from a short interval for grain growth of quartz during the low-*P*/high-*T* Ryoke metamorphism. The low-*P*/high-*T* metamorphism has been considered to be caused by the thermal effect due to the intrusion of the synkinematic granitoid magmas; a period of the high-*T* condition may be shorter than a few million years (Okudaira, 1996; Tirone and Ganguly, 2010). Alternatively, microstructural characteristics in metacherts suggest that grain pinning by second-phase minerals (Zener drag: e.g. Herwegh and Berger, 2004) prevented the growth of quartz grains. Second-phase contents as small as 2–3 vol.% are already sufficient to affect the quartz grain size (Song and Ree, 2007; M. Herwegh, personal communication).

The grain size of quartz in the chlorite-biotite zone metachert (sample 070523-12) varies significantly depending on different domains (Fig. 3b and Table 1). The quartz

grain size of domains of the quartz abundance similar to the chlorite zone sample is larger than that of the chlorite zone sample; the difference in their grain size must reflect their metamorphic grade. In the chlorite-biotite zone metachert, the modal abundance of quartz is lower in the domains of smaller quartz grain size, suggesting that there is a relationship between the volume fraction of second phases and the grain size of matrix quartz. The effect of second-phase minerals on the grain size of matrix mineral can be evaluated using Zener parameter that is a ratio of the grain size (μm) of second phases to the second phase volume fraction (Herwegh and Berger, 2004). The calculated Zener parameters for domains in metacherts are listed in Table 1; in the chlorite-biotite zone metachert, with decreasing values of the Zener parameter, the quartz grain sizes are toward smaller values, suggesting that grain pinning by second phases may have prevented the growth of quartz grains.

Furthermore, quartz grains in domains having many second phases (domain 1, Fig. 3c left side) are slightly elongated parallel to the tectonic foliation, compared to those in domains with less second phases (domain 3, Fig. 3c right side), suggesting that second-phase sheet silicates pin the quartz grain boundaries. Grain-boundary pinning forces the grain sizes to remain small and the fabric to deform under diffusion creep condition (e.g. Lisle, 1985a; Herwegh and Jenni, 2001; Krabbendam et al., 2003; Herwegh and Berger, 2004; Song and Ree, 2007).

3.2. Transition between dislocation creep and diffusion creep

At a constant temperature, the change in deformation mechanism from diffusion

creep to dislocation creep is controlled mainly by the grain size of quartz and/or flow stress (or strain rate): for a smaller grain size and/or lower stress/strain rate, diffusion creep is the dominant deformation mechanism. Assuming that the grain size of quartz is ~10 μm and pressure–temperature conditions are of the continental middle crust (~500 °C at 200–300 MPa) at a natural strain rate (10^{-14}–10^{-16} s^{-1}), quartz-rich rocks would deform mainly by diffusion creep. However, evidence of grain-size-sensitive deformation is rarely observed in naturally deformed rocks, even in ultramylonites (e.g. Fitz Gerald et al., 2006; Ishii et al., 2007).

The samples of upper greenschist to lower amphibolite facies metachert analyzed in the present study are metamorphic tectonites, but were not deformed in a shear zone; they may have formed under a lower strain rate or lower flow stress than did rocks in high-strain zones or shear zones.

In metachert samples, hydrous sheet silicates, i.e., chlorite, muscovite and biotite occur along quartz grain boundaries, having a strong preferred orientation with the basal planes parallel to the tectonic foliation. There is no chemical heterogeneity within each crystal. These observations suggest that they crystallized by dehydration reactions during the main low-*P*/high-*T* metamorphism, implying that fluids should be present during deformation to contribute to grain-boundary diffusion and grain growth, although amounts of fluids cannot be estimated.

Based on these observations, it suggests that if quartzose rocks deformed under the conditions of low- to medium-grade metamorphism at a lower strain rate or flow stress in a water-present environment, diffusion creep could be the dominant deformation

mechanism.

We tested this hypothesis by calculating stress values at different strain rates and varying grain sizes with temperatures. We calculated the grain size d of quartz during coarsening as part of normal grain growth, using the following relation (Joesten, 1983; Farver and Yund, 2000):

$$d = \left(\frac{8\gamma V}{\mathrm{R}T} \frac{D_G}{W} \Delta t + d_0^n \right)^{1/n}, \tag{4}$$

where the surface free energy $\gamma = 0.4$ J/m^2 (Parks, 1984), the growth exponent $n = 2$, the initial grain size $d_0 = 1$ μm, and the growth interval $\Delta t = 0.01$ Myr. Other parameters are the same of Eqs. (1) and (2). The growth interval is set to be that the variation of the quartz grain size calculated here is comparable with that in metacherts of the Ryoke metamorphic belt (Okudaira et al., 1995; this study), although there are uncertainties in temperature estimation (Fig. 8b). Theoretical considerations predict a value of $n = 2$ in a pure single-phase system, although empirical values of n are typically significantly greater than 2 (Farver and Yund, 2000). Given that the growth exponent is significantly greater than 2, the growth interval for quartz grains would be much longer than the value used here. Applying the estimated grain sizes to the flow law for grain-boundary diffusion creep (Coble creep), we obtained values of stress for grain-size-sensitive creep at strain rates of 10^{-12}, 10^{-14} and 10^{-16} s^{-1}.

The flow stresses at different strain rates calculated for dislocation creep decrease monotonically with increasing temperature, whereas the stresses for diffusion creep

decrease with increasing temperature in the conditions of smaller grain size (< a few micrometers) and lower temperature (<~300 °C), and increase at larger grain size and higher temperature (Fig. 8). In the conditions of smaller grain size and lower temperature, difference between the stress for diffusion creep and dislocation creep at a low strain rate (10^{-16} s^{-1}) is much larger than that at a high strain rate (10^{-12} s^{-1}). This difference in flow stress for the two creep mechanisms reflects a difference in the stress exponent between diffusion creep and dislocation creep; i.e. the difference in stress between the different strain rates is much larger for diffusion creep than for dislocation creep. In the conditions of larger grain size and higher temperature, flow stresses for diffusion creep increase with increasing grain size of quartz and then are greater than those for dislocation creep: the upper limit of temperature of which the stress for diffusion creep is lower than that for dislocation creep increases as the strain rate decreases (Fig. 8a).

Based on the results of previous studies (Toriumi et al., 1986; Toriumi, 1989; Okudaira et al., 1995) and this study, temperature of the transition from diffusion creep to dislocation creep in metacherts of the Ryoke metamorphic belt may be ~400–500 °C at the quartz grain size of several tens of micrometer (Fig. 8b): a low strain rate is suitable for the condition to form the metacherts. Consequently, at the condition of a water-present environment and a low strain rate or flow stress, low- to medium-grade metamorphic tectonites composed by very-fine-grained quartz could deform by diffusion creep.

4. Conclusions

In this study, we described microstructural and textural characteristics in the upper greenschist- to lower amphibolite-facies metacherts of the Cretaceous low-*P*/high-*T* Ryoke metamorphic belt, SW Japan. They are indicative of grain-size-sensitive flow (diffusion creep accompanied by grain-boundary sliding) rather than dislocation creep, possibly reflecting the relatively low strain rate or low flow stress compared with that in high-strain zones. Based on the results of the previous study that revealed dislocation creep as the dominant deformation mechanism in the higher grade metacherts and of this study, temperature and quartz grain size of the transition between diffusion creep and dislocation creep in metacherts of the Ryoke metamorphic belt may be ~400–500 °C and several tens of micrometer, respectively. The results of this study suggest the development of grain-size-sensitive flow in metamorphic tectonites at mid-crustal conditions, resulting in a significant decrease of the rocks strength of the continental middle crust.

Acknowledgements

We thank K. Ishii and O. Nishikawa for their helpful discussions during the course of this work. A. Nicolas and D.J. Prior are thanked for useful comments on the early version of the manuscript. The paper benefited substantially from detailed reviews by C. Delle Piane and M. Herwegh. M. Liu is thanked for his editorial handling of the manuscript. This study was supported financially by a Grant-in-Aid for Scientific Research (19540485) awarded to T. Okudaira by the Japan Society for the Promotion of

Science.

References

Barreiro, J.G., Lonardelli, I., Wenk, H.-R., Dresen, G., Rybacki, E., Ren, Y., Tomé, C.N., 2007. Preferred orientation of anorthite deformed experimentally in Newtonian creep. Earth and Planetary Science Letters 264, 188–207.

Behrmann, J.H., 1983. Microstructure and fabric transition in calcite tectonites from the Sierra Alhamilla (Spain). Geologische Rundschau 72, 605–618.

Behrmann, J.H., Mainprice, D., 1987. Deformation mechanisms in a high-temperature quartz feldspar mylonite: evidence for superplastic flow in the lower continental crust. Tectonophysics 140, 297–305.

Bestmann, M., Prior, D.J., 2003. Intragranular dynamic recrystallization in naturally deformed calcite marble: a case study by means of misorientation analysis. Journal of Structural Geology 25, 1597–1613.

De Bresser, J.H.P., Ter Heege, J.H., Spiers, C.J., 2001. Grain size reduction by dynamic recrystallization: can it result in major rheological weakening? International Journal of Earth Sciences 90, 28–45.

Delle Piane, C., Burlini, L., Kunze, K., 2009. The influence of dolomite on the plastic flow of calcite: Rheological, microstructural and chemical evolution during large strain torsion experiments. Tectonophysics 467, 145–166.

Dunnet, D., 1969. A technique of finite strain analysis using elliptical particles. Tectonophysics 7, 117–136.

Dunnet, D., Siddans, A.W.B., 1971. Non-random sedimentary fabrics and their modification by strain. Tectonophysics 12, 307–325.

Etheridge, M.A., Wilkie, J.C., 1979. Grainsize reduction, grain boundary sliding and the flow strength of mylonites. Tectonophysics 58, 159–178.

Farver, J., Yund, R., 1991. Oxygen diffusion in quartz: dependence on temperature and water fugacity. Chemical Geology 90, 55–70.

Farver, J., Yund, R., 2000. Silicon diffusion in a natural quartz aggregate: constraints on solution-transfer diffusion creep. Tectonophysics 325, 193–205.

Fitz Gerald J.D., Mancktelow, N.S., Pennacchioni, J., Kunze, K., 2006. Ultrafine-grained quartz mylonites from high-grade shear zones: Evidence for strong dry middle to lower crust. Geology 34, 369–372.

Fliervoet, T.F., White, S.H., 1995. Quartz deformation in a very fine grained quartzo-feldspathic mylonite: a lack of evidence for dominant grain boundary sliding deformation. Journal of Structural Geology 17, 1095–1109.

Fliervoet, T.F., White, S.H., Drury, M.R., 1997. Evidence for dominant grain-boundary sliding deformation in greenschist- and amphibolite-grade polymineralic ultramylonites from the Redbank Deformed Zone, Central Australia. Journal of Structural Geology 19, 1495–1520.

Fukui, A., Kano, K., 2007. Deformation process and kinematics of mélange in the Early Cretaceous accretionary complex of the Mino–Tamba Belt, eastern southwest Japan. Tectonics 26, TC2006, doi:10.1029/2006TC001945.

Goldsby, D.L., Kohlstedt, D.L., 2001. Superplastic deformation of ice: Experimental

obdservations. Journal of Geophysical Research 106B, 11017–11030.

Hara, I., 1962. Studies of the structure of the Ryoke metamorphic rocks of the Kasagi district, southwest Japan. Journal of Sciences of the Hiroshima University Series C 4, 163–224.

Heilbronner, R., Tullis, J., 2002. The effect of static annealing on microstructures and crystallographic preferred orientations of quartzites experimentally deformed in axial compression and shear. In: De Meer, S., Drury, M.R., De Bresser, J.H.P., Pencock, G.M. (Eds.), Deformation Mechanisms, Rheology and Tectonics: Current Status and Future Perspectives. Geological Society of London, Special Publications 200, pp. 191–218.

Herwegh, M., Jenni, A., 2001. Granular flow in polymineralic rocks bearing sheet silicates: new evidence from natural examples. Tectonophysics 332, 309–320.

Herwegh, M., Berger, A., 2004. Deformation mechanisms in second-phase affected microstructures and their energy balance. Journal of Structural Geology 26, 1483–1498.

Hirth, G., Kohlstedt, D.L., 1995. Experimental constraints on the dynamics of the partially molten upper mantle: 2. Deformation in the dislocation creep regime. Journal of Geophysical Research 100B, 15441–15449.

Ishii, K., Kanagawa, K., Shigematsu, N., Okudaira, T., 2007. High ductility of K-feldspar and development of granitic banded ultramylonite in the Ryoke metamorphic belt, SW Japan. Journal of Structural Geology 29, 1083–1098.

Jessell, M.W., 1988. Simulation of fabric development in recrystallized aggregates, II.

Example model runs. Journal of Structural Geology 10, 779–793.

Jiang, Z.T., Prior, D.J., Wheeler, J., 2000. Albite crystallographic preferred orientation and grain misorientation distribution in a low-grade mylonite: implications for granular flow. Journal of Structural Geology 22, 1663–1674.

Joesten, R., 1983. Grain growth and grain-boundary diffusion in quartz from the Christmas Mountains (Texas) contact aureole. American Journal of Science 283, 233–254.

Kamb, B.W., 1959. Ice petrofabric observations from Blue Glacier, Washington, in relation to theory and experiment. Journal of Geophysical Research 64B, 1891–1909.

Krabbendam, M., Urai, J.L., Vliet, L.J., 2003. Grain size stabilisation by dispersed graphite in a high-grade quartz-mylonite: an example from Naxos (Greece). Journal of Structural Geology 25, 855–866.

Kruse, R., Stünitz, H., 1999. Deformation mechanisms and phase distribution in mafic high-temperature mylonites from the Jotun Nappe, Southern Norway. Tectonophysics 303, 223–249.

Lisle, R.J., 1985a. The effect of composition and strain on quartz-fabric intensity in pebbles from a deformed conglomerate. Geologische Rundschau 74, 657–663.

Lisle, R.J., 1985b. The use of the orientation tensor for the description and statistical testing of fabrics. Journal of Structural Geology 7, 115–117.

Lister, G.S., Hobbs, B.E., 1980. The simulation of fabric development during plastic deformation and its application to quartzite: the influence of deformation history.

Journal of Structural Geology 2, 355–371.

Nadai, A., 1963. Theory of Flow and Fracture of Solid (vol. II). McGraw-Hill, New York.

Nakamura, D., 1995. Comparison and interpretation of graphitization in contact and regional metamorphic rocks. The Island Arc 4, 112–127.

Neumann, B., 2000. Texture development of recrystallized quartz polycrystals unraveled by orientation and misorientation characteristics. Journal of Structural Geology **22**, 1695–1711.

Okudaira, T., 1996. Temperature-time path for the low-pressure Ryoke metamorphism, Japan, based on chemical zoning in garnet. Journal of Metamorphic Geology 14, 427–440.

Okudaira, T., Takeshita, T., Hara, I., Ando, J., 1995. A new estimate of the conditions for transition from basal <*a*> to prism [*c*] slip in naturally deformed quartz. Tectonophysics 250, 31–46.

Okudaira, T., Beppu, Y., Yano, R., Tsuyama, M., Ishii, K., 2009. Mid-crustal horizontal shear zone in the forearc region of the mid-Cretaceous SW Japan arc, inferred from strain analysis of rocks within the Ryoke metamorphic belt. Journal of Asian Earth Sciences 35, 34–44.

Otani, M., Wallis, S., 2006. Quartz lattice preferred orientation patterns and static recrystallization: Natural examples from the Ryoke belt, Japan. Geology 34, 561–564.

Ozaki, M., Sangawa, A., Miyazaki, K., Nishioka, Y., Miyachi, Y., Takeuchi, K.,

Tagutschi, Y., 2000. Geology of the Nara District. Quad. Ser., Scale 1:50,000, Geological Survey of Japan, Tsukuba, 162 pp. (in Japanese with English abstract).

Parks, G.A., 1984. Surface and interfacial free energies of quartz. Journal of Geophysical Research 89B, 3997–4008.

Passchier, C.W., Trouw, R.A.J., 2005. Microtectonics. Springer-Verlag, Berlin.

Prior, D.J., Boyle, A.P., Brenker, F., Cheadle, M.C., Day, A., Lopez, G., Peruzzo, L., Potts, G.J., Reddy, S., Spiess, R., Timms, N.E., Trimby, P., Wheeler, J., Zetterstrom, L., 1999. The application of electron backscatter diffraction and orientation contrast imaging in the SEM to textural problems in rocks. American Mineralogist 84, 1741–1759.

Ramsay, J.G., Huber, M.L., 1983. The Techniques of Modern Structural Geology (vol. 1) Strain Analysis. Academic Press, London.

Rutter, E.H., Brodie, K.H., 2004. Experimental grain size-sensitive flow of hot-pressed Brazilian quartz aggregates. Journal of Structural Geology 26, 2011–2023.

Rutter, E.H., Casey, M., Burlini, L., 1994. Preferred crystallographic orientation development during the plastic and superplastic flow of calcite rocks. Journal of Structural Geology 16, 1431–1446.

Schmid, S.M., Boland, J.N., Paterson, M.S., 1977. Superplastic flow in fine grained limestone. Tectonophysics 43, 257–291.

Skemer, P., Katayama, I., Jiang, Z., Karato, S.-I., 2005. The misorientation index: Development of a new method for calculating the strength of lattice-preferred orientation. Tectonophysics 411, 157–167.

Song, W.J., Ree, J.-H., 2007. Effect of mica on the grain size of dynamically recrystallized quartz in a quartz–muscovite mylonite. Journal of Structural Geology 29, 1872–1881.

Storey, C.D., Prior, D.J., 2005. Plastic deformation and recrystallization of garnet: A mechanism to facilitate diffusion creep. Journal of Petrology 46, 2593–2613.

Stünitz, H., Fitz Gerald, J.D., 1993. Deformation of granitoids at low metamorphic grade, II. Granular flow in albite-rich mylonites. Tectonophysics 221, 299–324.

Takeshita, T., Wenk, H.-R., Lebensohn, R., 1999. Development of preferred orientation and microstructure in sheared quartzite: comparison of natural data and sumulated results. Tectonophysics 312, 133–155.

Tirone, M., Ganguly, J., 2010. Garnet composition as recorders of P–T-t history of metamorphic rocks. Gondwana Research, in press.

Toriumi, M., 1989. Microstructures of regional metamorphic rocks. In: Karato, S.-I., Toriumi, M. (Eds.), Rheology of Solids and of the Earth, Oxford University Press, Oxford, pp 319–337.

Toriumi, M., Teruya, J., Masui, M., Kuwahara, H., 1986. Microstructures and flow mechanisms in regional metamorphic rocks of Japan. Contributions to Mineralogy and Petrology 94, 54–62.

Toriumi, M., Masui, M., Mori, K., 1988. Strain in metacherts as determined from deformed shapes of radiolaria and Fry's method. Tectonophysics 145, 157–161.

Warren, J.M., Hirth, G., 2006. Grain size sensitive deformation mechanisms in naturally deformed peridotites. Earth and Planetary Science Letters 248, 438–450.

Wenk, H.-R., Canova, G., Molinari, A., Kocks, U.F., 1989. Viscoplastic modeling of texture development in quartzite. Journal of Geophysical Research 94, 17895–17906.

Wheeler, J., Prior, D., Jiang, Z., Spiess, R., Trimby, P., 2001. The petrological significance of misorientations between grains. Contributions to Mineralogy and Petrology 141, 109–124.

Wightman, R.H., Prior, D.J., Little, T.A., 2006. Quartz veins deformed by diffusion creep-accommodated grain boundary sliding during a transient, high strain-rate event in the Southern Alps, New Zealand. Journal of Structural Geology 28, 902–918.

Woodcock, N.H., Naylor, M.A., 1983. Randomness testing in three-dimensional orientation data. Journal of Structural Geology 5, 539–548.

Figure Captions

Fig. 1. Variations in effective viscosity with temperature, for dislocation creep and diffusion creep for various grain sizes. Viscosity was calculated for a strain rate of 10^{-14} s^{-1}.

Fig. 2. (a) Distribution of the Ryoke metamorphic belt, SW Japan and (b) geology of the Wazuka–Kasagi district (Ozaki et al., 2000; Okudaira et al., 2009). Sample localities are also shown. Inset: lower-hemisphere equal-area projection showing the orientations of the stretching lineation observed upon the schistosity within metacherts (open circles) and metapelites (open squares).

Fig. 3. Representative photomicrographs showing the microstructure of the analyzed metachert samples. (a) Sample 080429-04 (*XZ*-section) from the chlorite zone (left, plane-polarized light; right, cross-polarized light). Aligned, ellipsoidal radiolarian fossils define a weak foliation. Quartz grains within the radiolarian fossils are larger than those in the matrix. (b) Sample 070523-12 (*XZ*-section) from the chlorite–biotite zone (cross-polarized light). The photomicrographs show the microstructures in domains of different grain size (domains 1 and 3) where SEM-EBSD analyses were performed. (c) Back-scattered electron (BSE) images of domains 1 and 3 of sample 070523-12. Light gray: biotite or chlorite, medium gray: muscovite, dark gray: quartz.

Fig. 4. R_f–ϕ plots on the *XZ*-plane. Contours indicate the fields of expected R_f–ϕ plots for R_i = 1.5, 2.0, 2.5 and 3.0. R_s: strain ellipse defined by determining the family of θ-curves for which the $\theta = \pm 45°$ lines divide the data into two groups on each R_f–ϕ plot. n: number of data.

Fig. 5. Pole figures of quartz *c*-axis data. The measured quartz LPOs for *XZ*-sections are presented on lower-hemisphere, equal-area stereographic projections in the structural reference frame, with the foliation (*XY* plane) being vertical and striking E–W, and the lineation (*X* direction) being horizontal, trending E–W. In this figure, the contour interval is 2σ and the significance level is 3σ (i.e. Kamb contouring). The domains of ≥2σ (i.e. twice the standard deviation for a random distribution) indicate statistically significant difference from a uniform distribution (Kamb, 1959). n: number of data.

Fig. 6. Distribution frequency of misorientation angles for each of the analyzed samples. Data calculated for 1° bins are plotted as a normalized histogram. Solid lines represent the theoretical curve for the distribution of uncorrelated misorientation angles for a random fabric (Wheeler et al., 2001).

Fig. 7. Relationship between the average grain size of quartz grains and fabric strength parameters: (a) the M-index and (b) Lisle's (1985b) fabric intensity. Open squares: sample 080429-04; solid circles: sample 070523-12. Numbers next to solid circles indicate the domain analyzed by SEM-EBSD. Horizontal bars represent the standard deviation (1σ).

Fig. 8. (a) Variations in flow stress with increasing quartz grain size for diffusion creep and dislocation creep at strain rates of 10^{-12}, 10^{-14} and 10^{-16} s^{-1}. (b) Variation of the quartz grain size calculated to estimate flow stress for diffusion creep. The variation was set to be comparable with that in metacherts of the Ryoke metamorphic belt (open circles: Okudaira et al., 1995; solid circles: this study), although there are uncertainties in temperature estimation. Since the dominant deformation mechanisms of metacherts

denoted by solid circles and by open circles are grain-size-sensitive creep and dislocation creep, respectively, temperature and quartz grain size of the transition between diffusion creep and dislocation creep in metacherts of the Ryoke metamorphic belt may be ~400–500 °C and several tens of micrometer, respectively.

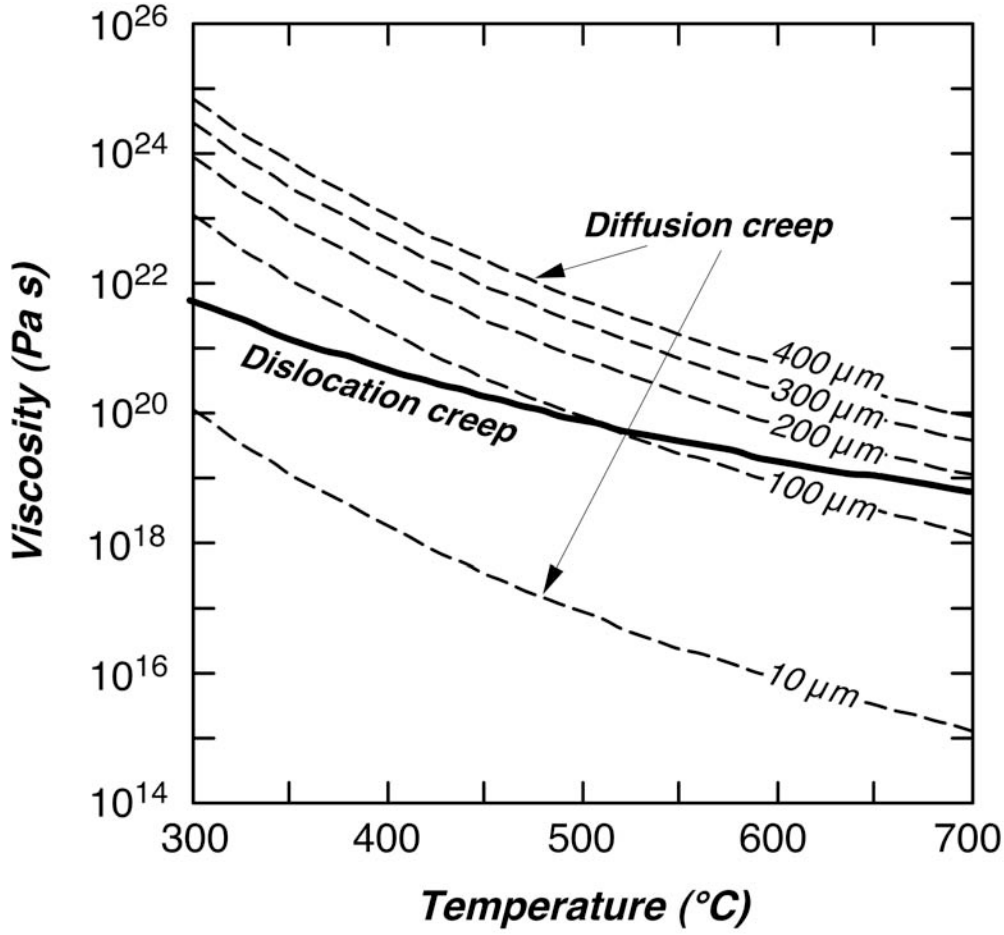

Fig. 1 (Okudaira et al.)

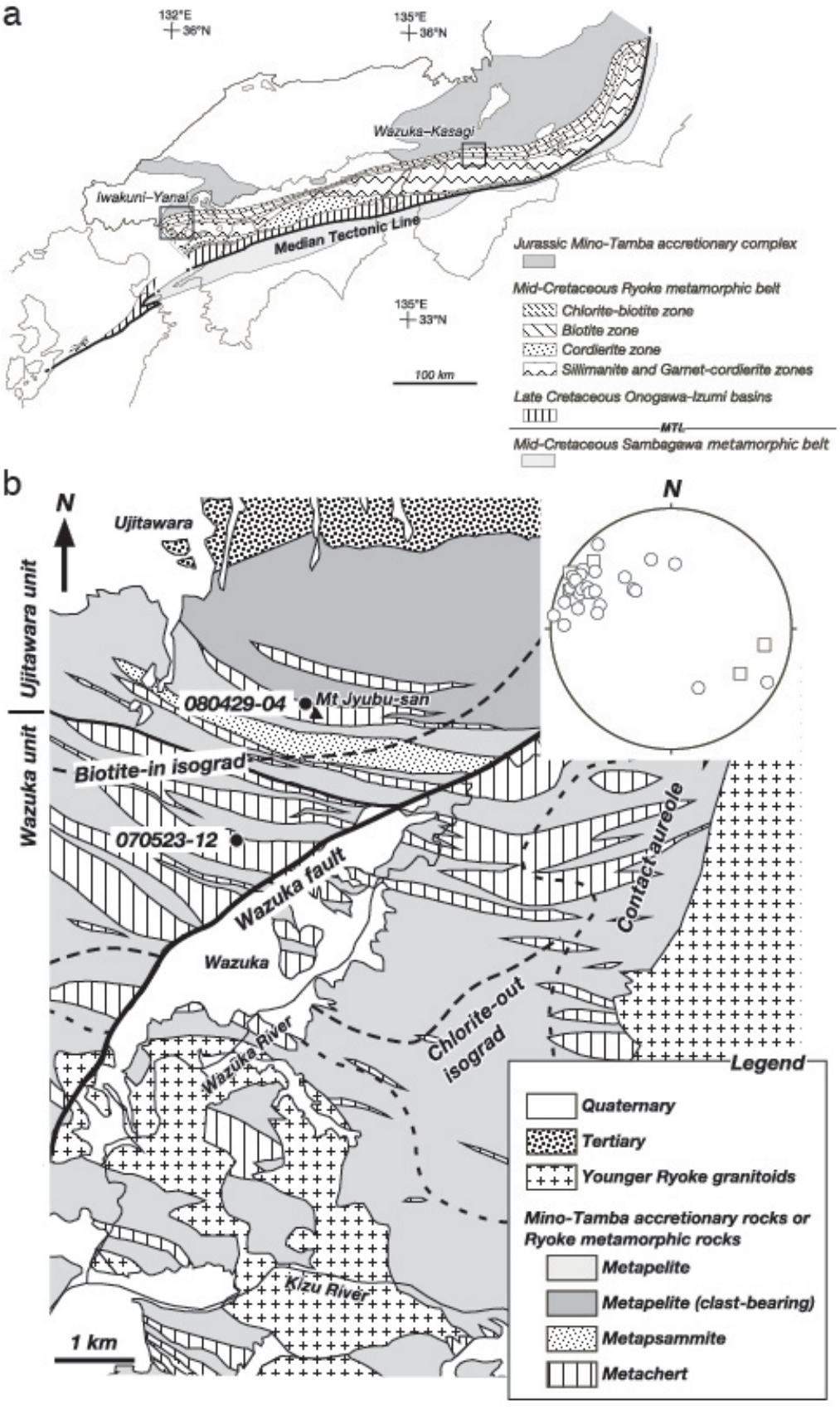

Fig. 2 (Okudaira et al.)

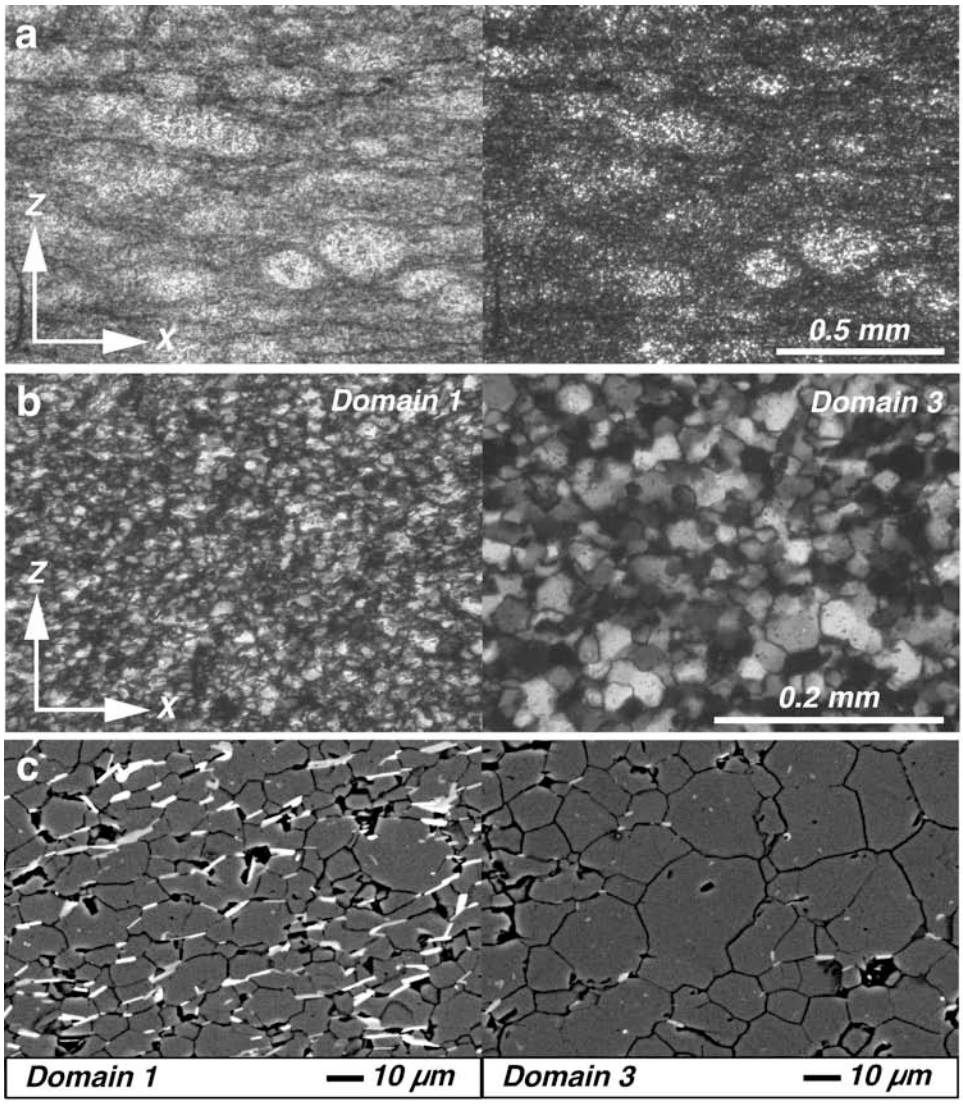

Fig. 3 (Okudaira et al.)

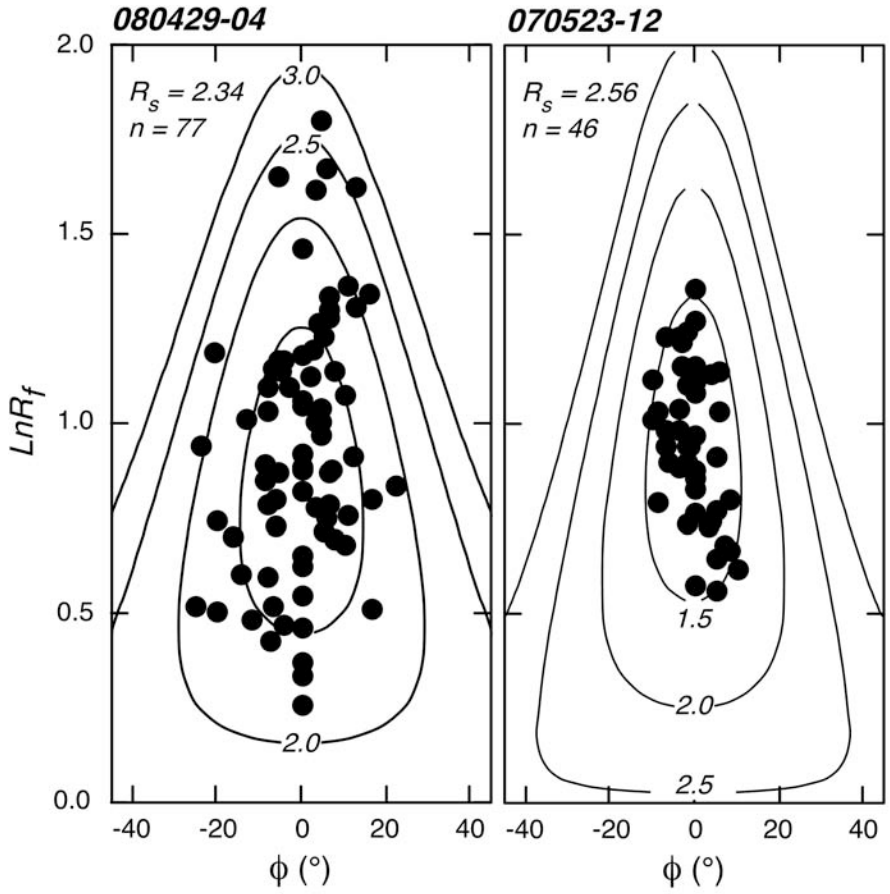

Fig. 4 (Okudaira et al.)

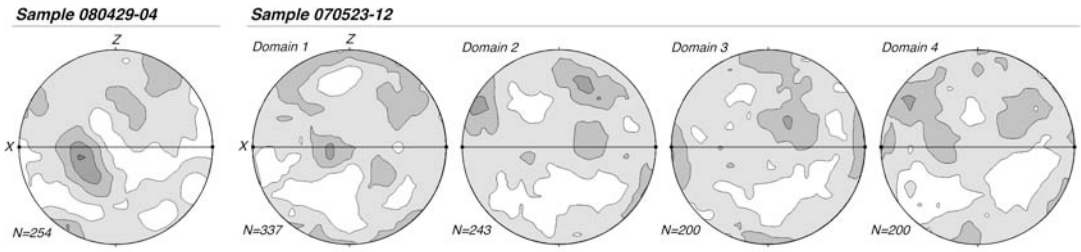

Fig. 5 (Okudaira et al.)

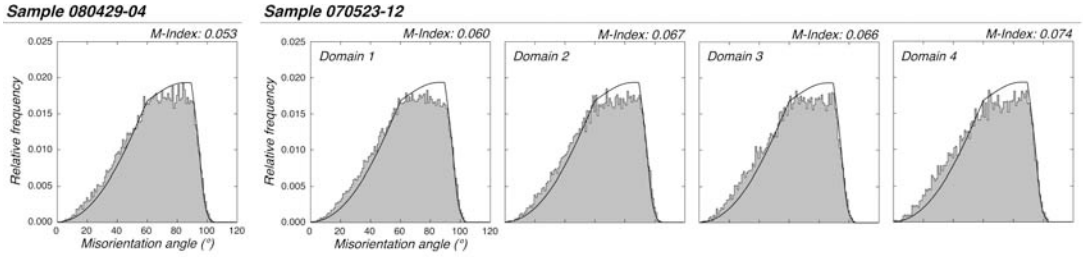

Fig. 6 (Okudaira et al.)

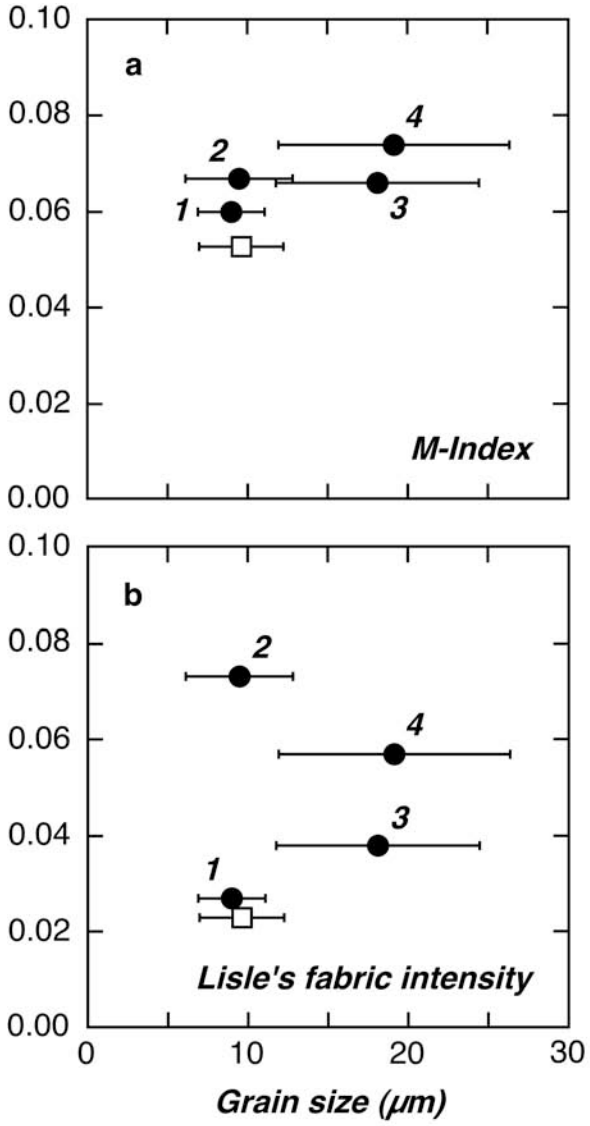

Fig. 7 (Okudaira et al.)

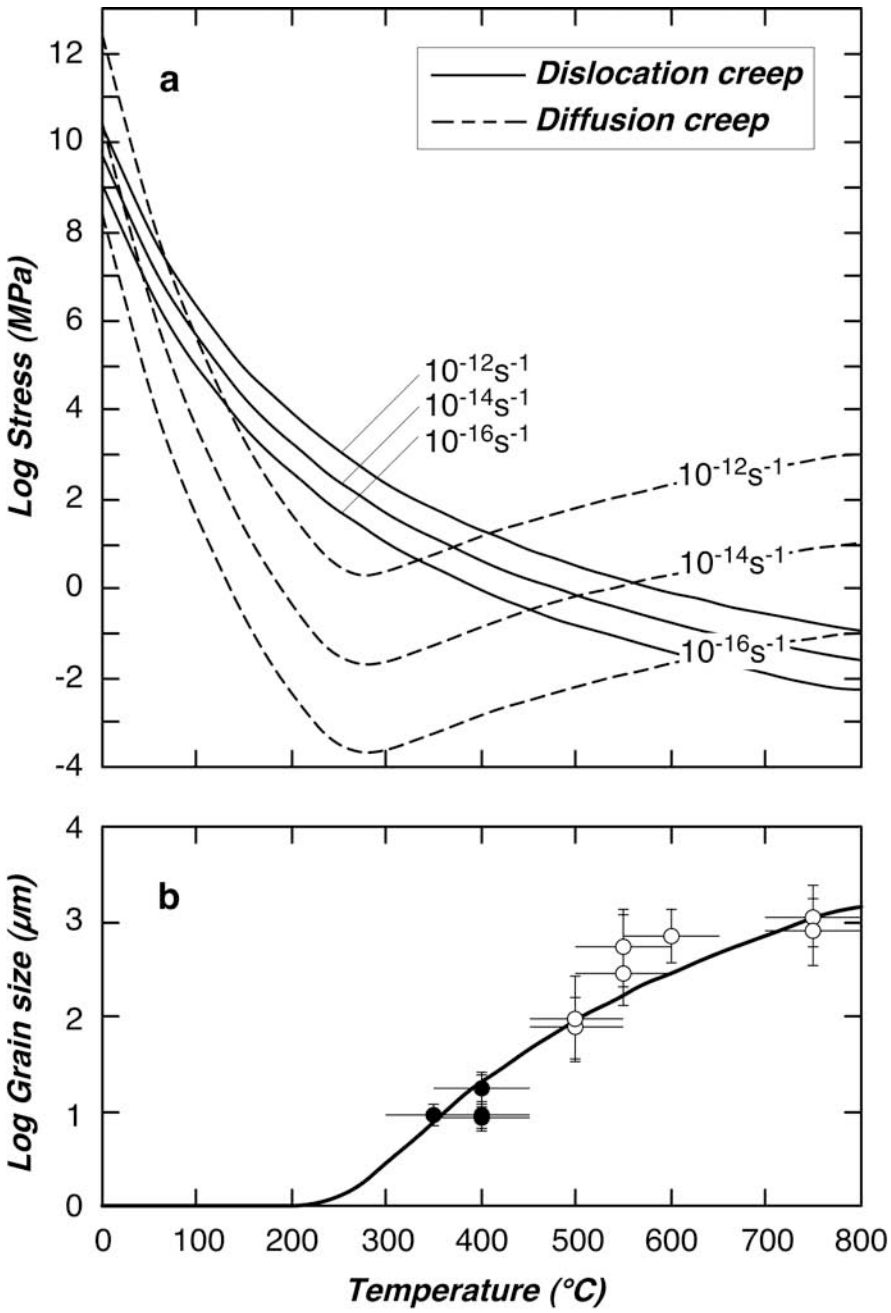

Fig. 8 (Okudaira et al.)